Organosilicon Compounds as Adult T-Cell Leukemia Cell Proliferation Inhibitors

Masaharu Nakamura,[a] Yotaro Matsumoto,[a] Masaaki Toyama,[b] Masanori Baba,[b] and Yuichi Hashimoto*,[a]

[a] *Institute of Molecular and Cellular Biosciences, The University of Tokyo; 1–1–1 Yayoi, Bunkyo-ku, Tokyo 113–0032, Japan: and* [b] *Division of Antiviral Chemotherapy, Center for Chronic Viral Diseases, Graduate School of Medical and Dental Sciences, Kagoshima University; 8–35–1 Sakuragaoka, Kagoshima 890–8544, Japan.*
Received September 23, 2012; accepted November 2, 2012

Aggressive forms of adult T-cell leukemia (ATL) respond poorly to conventional anticancer chemotherapy, and new lead compounds are required for the development of drugs to treat this fatal disease. Recently, we developed ATL cell-selective proliferation inhibitors based on a tetrahydrotetramethylnaphthalene (TMN) skeleton 1, and here we report the design and synthesis of silicon analogs of TMN derivatives. Among them, compound 13 showed the most potent growth-inhibitory activity towards the ATL cell line S1T, though its selectivity for S1T over the non-ATL cell line MOLT-4 was only moderate. This result, as well as computational studies, suggests that sila-substitution (C/Si exchange) is useful for structure optimization of these inhibitors.

Key words silicon; adult T-cell leukemia; tetrahydrotetramethylnaphthalene skeleton; T-lymphotropic virus type 1; sila-substitution

Adult T-cell leukemia (ATL), an aggressive neoplasm of mature helper T cells, is caused by human T-lymphotropic virus type 1 (HTLV-1) infection.[1,2] Epidemiological studies indicate that approximately 15 to 20 million HTLV-1 carriers exist throughout the world, with endemic areas in Japan, the Caribbean, and Africa.[3] In Japan, the number of HTLV-1 carriers is estimated to be 1.2 million, and more than 700 cases of ATL are diagnosed every year.[4] Since conventional anticancer chemotherapy active against other lymphoid malignancies has proved to be ineffective for treating aggressive types of ATL, it is important to find or design superior lead compounds for the development of drugs to treat this fatal disease.[5–7]

Recently, we have succeeded in the development of ATL cell-selective proliferation inhibitors with a tetrahydrotetramethylnaphthalene (TMN) skeleton. Among them, several ketone compounds, including 2-acetyl-5,6,7,8-tetrahydro-5,5,8,8-tetramethylnaphthalene (**1**) (Fig. 1), exhibited ATL cell-selective growth-inhibitory activity.[8,9] Furthermore, sila-substitution (C/Si exchange) of existing drugs is an established approach to find new drug candidates that have beneficial biological properties and a clear intellectual property position. Several organosilicon agents have advanced to clinical studies.[10]

In the present paper, we report the synthesis and structure–activity relationships of silanediol, which is an isostere of ketone[11] (Fig. 2), and silanol derivatives of our TMN-based inhibitors (Fig. 3). We also describe the results of a computational study of these compounds.

Results and Discussion

Molecular Design and Computational Studies Our previous structure–activity relationship studies of 2-acetyl-5,6,7,8-tetrahydro-5,5,8,8-tetramethylnaphthalene (**1**) for ATL cell-selective proliferation-inhibiting activity suggested that the enol form of **1** is the active form.[8] Therefore, we designed a number of silanol and silanediol derivatives **5**–**9**, as well as the carba-control compound **10**. Silanediol has been reported to exist predominantly in diol form, while its carba-analog exists predominantly in carbonyl form[11] (Fig. 2).

First, we performed computational studies to examine the similarities and differences between sila- and carba-analogs. Generally, silicon has a longer bond distance than carbon, and its electronegativity is small. Next, we focused on the designed compounds **8** and **10** (Figs. 4, 5). Structure optimizations were performed at the M06/6-31+G* level of theory with the Gaussian 09 program package.[12] As shown in Fig. 4, due to the different covalent radii of carbon and silicon, the silicon compound **8** differs in size and shape from the carbon analogue **10**, though the electrostatic potentials of **8** and **10** are very similar (Fig. 5). Therefore, we examined the ATL cell-inhibitory activity of various sila- and carba-analogs.

Chemistry Compounds **1**–**13** were prepared by usual organic synthetic methods as illustrated in Chart 1. Compound **1** was prepared according to the reported method.[8] The silandiol derivatives **5** and **6** were synthesized as follows. Compound **2**, which was prepared as reported,[13] was converted by means

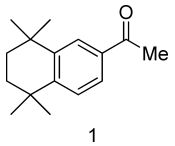

1

Fig. 1. Structure of 2-Acetyl-5,6,7,8-tetrahydro-5,5,8,8-tetramethylnaphthalene (**1**)

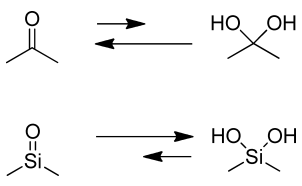

Fig. 2. Comparison of the Hydration Equilibrium for Ketone and Silanone (Silanediol) Moieties

The authors declare no conflict of interest.

* To whom correspondence should be addressed. e-mail: hashimot@iam.u-tokyo.ac.jp

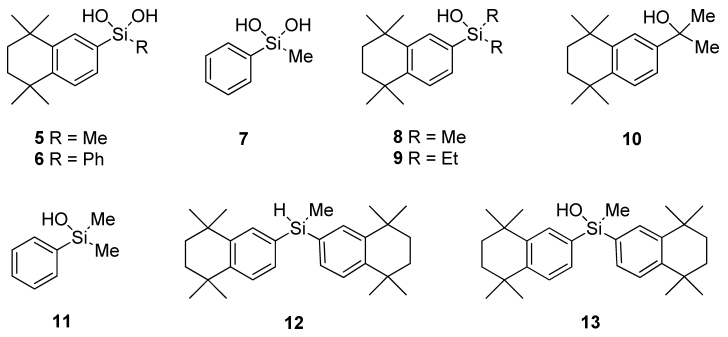

Fig. 3. Chemical Structures of Compounds **5**–**13**

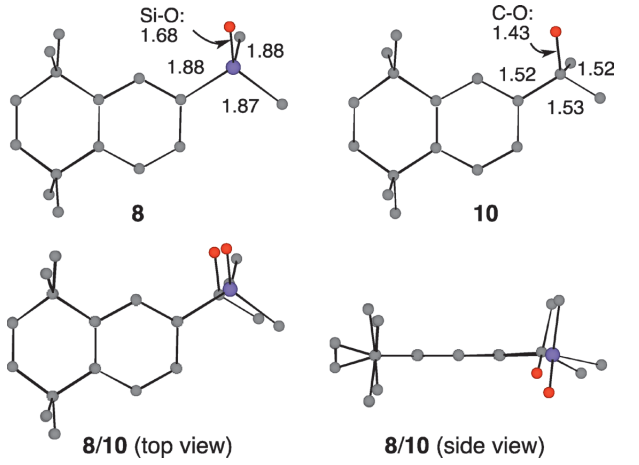

Fig. 4. Superpositions of the Calculated Structures of Compounds **8** and **10** Obtained by Geometry Optimizations

Hydrogen atoms are omitted for clarity.

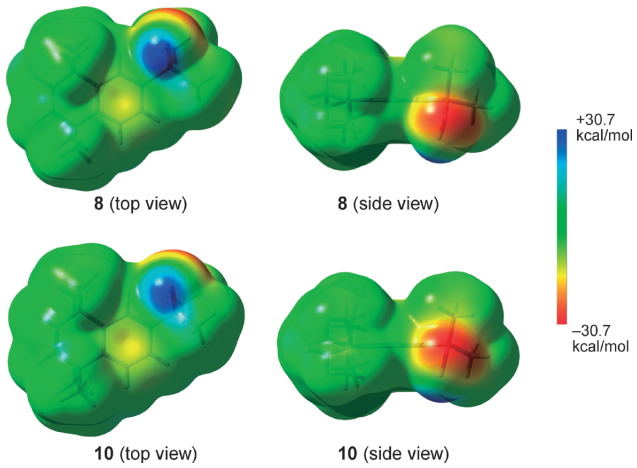

Fig. 5. Electrostatic Potential Field Maps of Compounds **8** and **10**

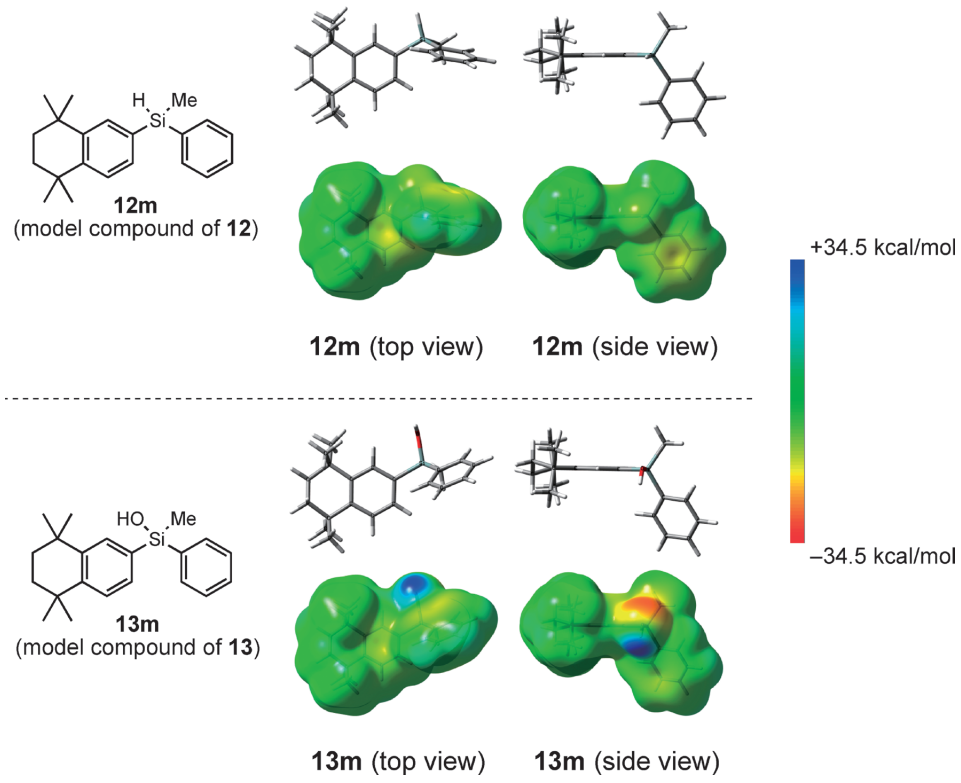

Fig. 6. Electrostatic Potential Field Maps of the Compounds **12** and **13**

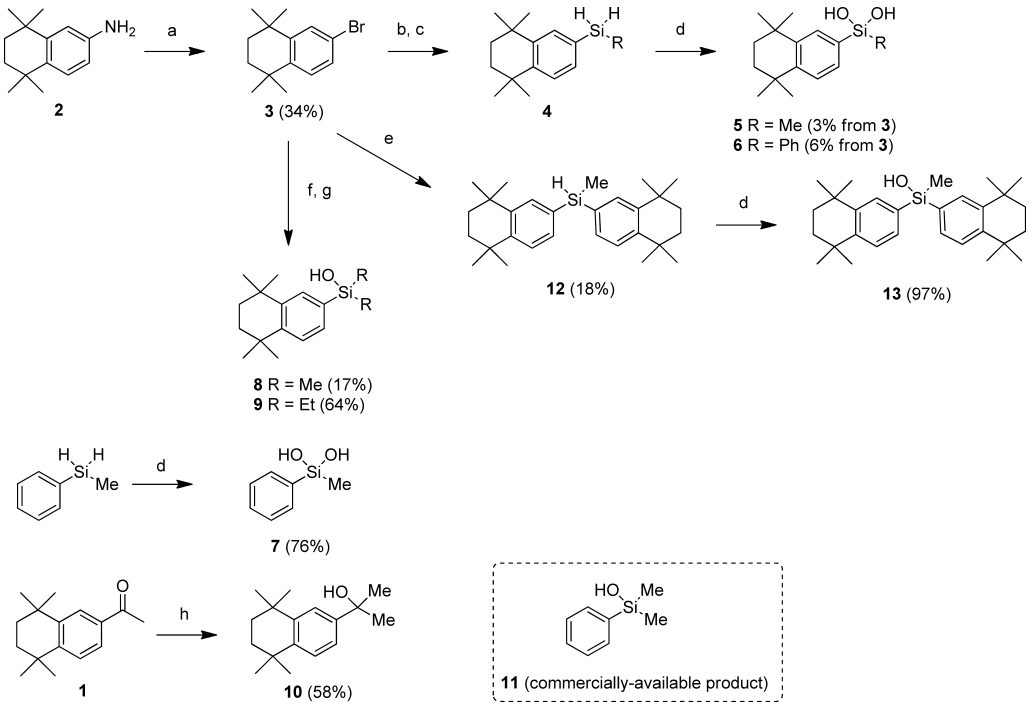

a) $NaNO_3$, HBr aq, CuBr (b) *i*-PrMgBr–LiCl, tetrahydrofuran (THF), $RSiCl_3$ (R= Me, Ph) (c) LAH, THF (d) Pd–C, 1,4-dioxane (e) *n*-BuLi–hexane, THF, $MeSiCl_3$ (f) *n*-BuLi–hexane, THF, Me_2SiCl_2 (R=Me, Et) (g) NaOH aq (h) MeMgBr, THF.

Chart 1

of the Sandmeyer reaction to the bromo derivative **3**. This was treated with *n*-butyllithium (*n*-BuLi), and then reacted with methyltrichlorosilane or phenyltrichlorosilane. The reaction product was reduced with lithium aluminium hydride (LAH), and oxidized with Pd/C to give silanediol derivatives **5** and **6**. The silanol derivatives **8**, **9**, **11** and **13** were synthesized in an analogous manner. Tertiary alcohol **10** was prepared by the reaction of methylmagnesium bromide (MeMgBr) with **1**.

Cell Biological Assays For screening of ATL cell-selective inhibitors, two cell lines were adopted: S1T established from acute-type ATL[6,14] and MOLT-4 established from HTLV-1- negative T-cell leukemia. Chemicals that inhibit proliferation of S1T cells, but not MOLT-4 cells, might be suitable lead compound(s) for the development of drugs to treat ATL. The effects of compounds **5**–**13** on the growth and viability of S1T and MOLT-4 cells were examined. S1T and MOLT-4 cells were incubated in the absence or presence of various concentrations of test compounds for 4 d, then the viable cell number was determined by the 3-(4,5-dimethylthiazol-2-yl)-2,5-diphenyltetrazolium bromide (MTT) method, and IC_{50} values were calculated. The results are shown in Table 1.

Structure–Activity Relationships Compound **1** showed S1T cell-selective proliferation-inhibitory activity with a selectivity index (SI: IC_{50} value for MOLT-4 cells/IC_{50} value for S1T cells) value of 9.6. Silanediol **5** showed weaker activity toward S1T cells, but with retention of activity toward MOLT-4 cells, resulting in loss of cell type selectivity (SI value of 1.1). The substitution of a methyl group for the phenyl group, that is, compound **6**, increased the growth-inhibitory activity towards both S1T and MOLT-4 cells, and the SI value was higher than that of **5** (SI value of 1.7). Compound **7**, in which the TMN skeleton was replaced with a benzene ring, was inactive (IC_{50} >100). Silanol **8** showed activity and selectivity comparable to that of silanediol **5**. The substitution of a methyl group for the ethyl group, that is, compound **9**, resulted in a very slight enhancement of the growth-inhibitory activity. The corresponding carbon compound of **8**, that is, tertiary alcohol **10**, showed about the same activity as **8** toward S1T cells. This result suggests that silanol can be used as a bioisostere of tertiary alcohol. Like compound **7**, compound **11** was inactive (IC_{50} >100). The tetramethylcyclohexane moiety of the above-mentioned compounds seems to be essential for the activity. Compound **13** showed the highest growth-inhibitory activity towards both S1T and MOLT-4 cells and the highest S1T selectivity (SI value of 2.0) among the silicon compounds in this study. Deletion of the hydroxyl group of **13**, that is, compound **12**, resulted in loss of activity (IC_{50} >100). Thus, it appears that the hydroxyl moiety is important for the

Table 1. Anti-proliferative Activity of Compounds **1** and **5**–**13** against S1T and MOLT-4 Cells

Compounds	IC_{50} (μM)		SI[a]
	S1T	MOLT-4	
1[b]	6.9	66.0	9.6
5	5.63	63.1	1.1
6	23.2	40.4	1.7
7	>100	>100	—
8	38.7	48.0	1.2
9	28.2	37.7	1.3
10	35.7	73.8	2.1
11	>100	>100	—
12	>100	>100	—
13	6.3	12.8	2.0

a) SI=selectivity index (IC_{50} value for MOLT-4 cells/IC_{50} value for S1T cells). *b*) Values taken from the literature.[8]

growth-inhibitory activity.

The electrostatic potentials of **12m** and **13m** (model compounds of **12**, **13**, respectively) were calculated. As shown in Fig. 6, the hydroxyl group impacts significantly on the electron density pattern and electrostatic potential.

Conclusion

We designed silicon analogs of various TMN derivatives that we had previously found to show ATL cell-selective proliferation-inhibitory activity, based on computational studies. Among the synthesized compounds, **13** showed the most potent growth-inhibitory activity towards S1T cells, though the selectivity over non-ATL MOLT-4 cells was only moderate (SI value of 2.0). These results suggest that sila-substitution (C–Si exchange) is a useful approach for structure optimization of these inhibitors. The next requirement is to improve the selectivity for ATL cells.

Experimental

General Comments ^{1}H-NMR spectra were recorded on a JEOL JNM-GX500 (500 MHz) spectrometer. Chemical shifts are expressed in parts per million relative to tetramethylsilane. Mass spectra were recorded on a JEOL JMS-DX303 spectrometer. Melting points were determined on a MP-J3 melting point apparatus (Yanaco, Japan).

Dimethyl(phenyl)silanol **11** was purchased from Wako Pure Chemical Industries, Ltd. (Japan).

Spectral Data for Compounds 3–13 6-Bromo-1,1,4,4-tetramethyl-1,2,3,4-tetrahydronaphthalene (**3**): Colorless oil. ^{1}H-NMR (500 MHz, $CDCl_3$) δ: 7.40 (1H, d, J=1.9 Hz), 7.22 (1H, dd, J=1.9, 8.5 Hz), 7.16 (1H, d, J=8.5 Hz), 1.67 (4H, s), 1.26 (6H, s), 1.25 (6H, s). ^{13}C-NMR (500 MHz, $CDCl_3$) δ: 147.41, 143.87, 129.43, 128.64, 128.46, 119.35, 34.87, 34.83, 34.48, 34.08, 31.87, 31.73. MS (FAB+) m/z: 268 ($M+H^+$).

Methyl(5,5,8,8-tetramethyl-5,6,7,8-tetrahydronaphthalen-2-yl)silanediol (**5**): White paste. ^{1}H-NMR (500 MHz, $CDCl_3$) δ: 7.60 (1H, s), 7.40 (1H, s), 7.32 (1H, s), 2.98 (2H, s), 1.68 (4H, s), 1.29 (6H, s), 1.28 (6H, s), 0.39 (3H, s). ^{13}C-NMR (500 MHz, $CDCl_3$) δ: 147.31, 144.36, 132.66, 131.85, 130.51, 126.16, 35.11, 34.93, 34.34, 34.18, 31.84, 31.72. High resolution (HR)-MS (FAB+) m/z: Calcd for $C_{15}H_{24}O_2SiLi$ 271.1706, Found 271.1693 ($M+Li^+$).

Phenyl(5,5,8,8-tetramethyl-5,6,7,8-tetrahydronaphthalen-2-yl)silanediol (**6**): White solid. mp 98–100°C. ^{1}H-NMR (500 MHz, $CDCl_3$) δ: 7.70 (2H, d, J=6.7 Hz), 7.66 (1H, s), 7.44–7.31 (4H, m), 7.30 (1H, d, J=8.0 Hz), 1.68 (4H, s), 1.27 (6H, s), 1.26 (6H, s). ^{13}C-NMR (500 MHz, $CDCl_3$) δ: 147.50, 144.35, 134.54, 134.45, 134.35, 132.75, 131.34, 130.66, 130.36, 127.90, 126.16, 35.10, 34.93, 34.36, 34.18, 31.83, 31.70. HR-MS (FAB+) m/z: Calcd for $C_{20}H_{26}O_2SiLi$ 333.1862, Found 333.1872 ($M+Li^+$).

Methyl(phenyl)silanediol (**7**): White solid. mp 83–84°C (lit. 85–86°C). ^{1}H-NMR (500 MHz, $CDCl_3$) δ: 7.61 (2H, d, J=7.9 Hz), 7.42 (1H, d, J=6.7 Hz), 7.37–7.35 (2H, m), 3.41 (2H, s), 0.38 (3H, s). ^{13}C-NMR (500 MHz, $CDCl_3$) δ: 136.03, 133.46, 130.29, 127.96, −1.80. HR-MS (FAB+) m/z: Calcd for $C_7H_{10}O_2Si$ 154.0450, Found 154.0443 (M^+).

Dimethyl(5,5,8,8-tetramethyl-5,6,7,8-tetrahydronaphthalen-2-yl)silanol (**8**): White solid. mp 57–59°C. ^{1}H-NMR (500 MHz, $CDCl_3$) δ: 7.55 (1H, s), 7.35 (1H, d, J=7.9 Hz), 7.33 (1H, d, J=7.9 Hz), 1.70 (4H, s), 1.30 (6H, s), 1.29 (6H, s), 0.40 (6H, s). ^{13}C-NMR (500 MHz, $CDCl_3$) δ: 146.60, 144.23, 135.54, 131.47, 130.20, 126.06, 35.19, 35.01, 34.32, 34.21, 31.90, 31.77, 0.00. HR-MS (FAB+) m/z: Calcd for $C_{16}H_{26}OSi$ 262.1753, Found 262.1749 (M^+).

Diethyl(5,5,8,8-tetramethyl-5,6,7,8-tetrahydronaphthalen-2-yl)silanol (**9**): Colorless oil. ^{1}H-NMR (500 MHz, $CDCl_3$) δ: 7.51 (1H, s), 7.31 (2H, m), 1.68 (4H, s), 1.29 (6H, s), 1.28 (6H, s), 1.03 (6H, t, J=7.9 Hz), 0.85 (4H, q, J=7.9 Hz). ^{13}C-NMR (500 MHz, $CDCl_3$) δ: 146.32, 144.03, 133.64, 131.97, 130.55, 125.90, 35.15, 35.01, 34.26, 34.12, 31.88, 31.73, 6.67, 6.34. HR-MS (FAB+) m/z: Calcd for $C_{18}H_{30}OSi$ 290.2066, Found 290.2061 (M^+).

Dimethyl(5,5,8,8-tetramethyl-5,6,7,8-tetrahydronaphthalen-2-yl)silanol (**10**): Pale yellow solid. mp 89–90°C. ^{1}H-NMR (500 MHz, $CDCl_3$) δ: 7.44 (1H, d, J=1.8 Hz), 7.27 (1H, dd, J=1.8, 7.9 Hz), 7.21 (1H, d, J=7.9 Hz), 1.68 (4H, s), 1.57 (6H, s), 1.29 (6H, s), 1.28 (6H, s). ^{13}C-NMR (500 MHz, $CDCl_3$) δ: 145.97, 144.57, 143.23, 126.26, 122.27, 121.82, 72.46, 35.23, 35.08, 34.40, 33.98, 31.90, 31.84, 31.6. HR-MS (FAB+) m/z: Calcd for $C_{17}H_{26}O$ 246.1984, Found 246.1972 (M^+).

Methylbis(5,5,8,8-tetramethyl-5,6,7,8-tetrahydronaphthalen-2-yl)silane (**12**): White solid. mp 96–97°C. ^{1}H-NMR (500 MHz, $CDCl_3$) δ: 7.51 (2H, s), 7.31 (2H, s), 7.30 (2H, s), 4.88 (1H, q, J=3.7 Hz), 1.67 (8H, s), 1.27 (12H, s), 1.26 (12H, s), 0.59 (3H, d, J=3.7 Hz). ^{13}C-NMR (500 MHz, $CDCl_3$) δ: 146.17, 144.15, 133.29, 131.94, 131.81, 126.02, 35.18, 35.04, 34.27, 34.17, 31.87, 31.76, −4.78. HR-MS (FAB+) m/z: Calcd for $C_{29}H_{41}Si$ 417.2978, Found 417.2976 ($M-H^+$). Calcd for $C_{29}H_{42}Si$ 418.3056, Found 418.3035 (M^+).

Methylbis(5,5,8,8-tetramethyl-5,6,7,8-tetrahydronaphthalen-2-yl)silanol (**13**): White solid. mp 131–132°C. ^{1}H-NMR (500 MHz, $CDCl_3$) δ: 7.58 (2H, s), 7.36 (2H, d, J=7.9 Hz), 7.31 (2H, d, J=7.9 Hz), 1.68 (8H, s), 1.28 (12H, s), 1.27 (12H, s), 0.64 (3H, s). ^{13}C-NMR (500 MHz, $CDCl_3$) δ: 146.61, 144.11, 133.74, 132.40, 131.03, 125.97, 35.18, 35.01, 34.31, 34.18, 31.88, 31.74, −1.09. HR-MS (FAB+) m/z: calcd for $C_{29}H_{42}OSi$ 434.3005, Found 434.3001 (M^+).

Computational Methods All calculations were carried with the Gaussian 09 program package. Geometry optimization and vibrational analysis were performed at the M06/6-31+G* level of theory. All stationary points were optimized without any symmetry assumptions, and characterized by normal coordinate analysis at the same level of the theory (number of imaginary frequencies, NIMAG, 0 for minima).

Acknowledgments The work described in this paper was partially supported by Grant-in-Aid for Scientific Research from the Ministry of Education, Culture, Sports, Science and Technology of Japan, and a Grant from the Japan Society for the Promotion of Science.

References

1) Uchiyama T., Yodoi J., Sagawa K., Takatsuki K., Uchino H., *Blood*, **50**, 481–492 (1977).
2) Tamiya S., Matsuoka M., Etoh K., Watanabe T., Kamihira S., Yamaguchi K., Takatsuki K., *Blood*, **88**, 3065–3073 (1996).
3) Edlich R. F., Arnette J. A., Williams F. M., *J. Emerg. Med.*, **18**, 109–119 (2000).
4) Takatsuki K., *Retrovirology*, **2**, 16 (2005).
5) Taylor G. P., Matsuoka M., *Oncogene*, **24**, 6047–6057 (2005).
6) Baba M., Okamoto M., Hamasaki T., Horai S., Wang X., Ito Y., Suda Y., Arima N., *J. Virol.*, **82**, 3843–3852 (2008).

7) Uozumi K., *J. Clin. Exp. Hematop.*, **50**, 9–25 (2010).
8) Nakamura M., Hamasaki T., Tokitou M., Baba M., Hashimoto Y., Aoyama H., *Bioorg. Med. Chem.*, **17**, 4740–4746 (2009).
9) Hamasaki T., Toyama M., Aoyama H., White Y., Okamoto M., Arima N., Hashimoto Y., Baba M., *Anticancer Res.*, **31**, 2241–2247 (2011).
10) Showell G. A., Mills J. S., *Drug Discov. Today*, **8**, 551–556 (2003).
11) Meanwell N. A., *J. Med. Chem.*, **54**, 2529–2591 (2011).
12) Frisch M. J., Trucks G. W., Schlegel H. B., Scuseria G. E., Robb M. A., Cheeseman J. R., Montgomery J. A. Jr., Vreven T., Kudin K. N., Burant J. C., Millam J. M., Iyengar S. S., Tomasi J., Barone V., Mennucci B., Cossi M., Scalmani G., Rega N., Petersson G. A., Nakatsuji H., Hada M., Ehara M., Toyota K., Fukuda R., Hasegawa J., Ishida M., Nakajima T., Honda Y., Kitao O., Nakai H., Klene M., Li X., Knox J. E., Hratchian H. P., Cross J. B., Bakken V., Adamo C., Jaramillo J., Gomperts R., Stratmann R. E., Yazyev O., Austin A. J., Cammi R., Pomelli C., Ochterski J. W., Ayala P. Y., Morokuma K., Voth G. A., Salvador P., Dannenberg J. J., Zakrzewski V. G., Dapprich S., Daniels A. D., Strain M. C., Farkas O., Malick D. K., Rabuck A. D., Raghavachari K., Foresman J. B., Ortiz J. V., Cui Q., Baboul A. G., Clifford S., Cioslowski J., Stefanov B. B., Liu G., Liashenko A., Piskorz P., Komaromi I., Martin R. L., Fox D. J., Keith T., Al-Laham M. A., Peng C. Y., Nanayakkara A., Challacombe M., Gill P. M. W., Johnson B., Chen W., Wong M. W., Gonzalez C., Pople J. A., Gaussian, Inc., Wallingford CT, *Gaussian 09* (Revision-A.01), Gaussian, Inc., Pittsburgh, PA, 2009.
13) Kagechika H., Kawachi E., Hashimoto Y., Himi T., Shudo K., *J. Med. Chem.*, **31**, 2182–2192 (1988).
14) Arima N., Molitor J. A., Smith M. R., Kim J. H., Daitoku Y., Greene W. C., *J. Virol.*, **65**, 6892–6899 (1991).